Mossbauer Study of the Hematite Phase Formed during Synthesis of Ferri-Diopsides

A. VAN ALBOOM,* E. DE GRAVE,† AND R. E. VANDENBERGHE

*Laboratory of Magnetism, University of Gent, Proeftuinstraat 86,
B-9000 Gent, Belgium*

The hematite phase, which is formed in the process of synthesizing ferri-diopsides with iron contents exceeding the solubility limit, has been studied by ^{57}Fe Mössbauer spectroscopy at variable temperatures between 80 and 900 K, in both ascending and descending sequences. The temperature variations of the hyperfine parameters were derived and interpreted. The Morin-transition temperature was found to be unusually high, i.e., $\approx$350 K, and possible explanations for this feature are discussed. © 1991 Academic Press, Inc.

1. Introduction

In the course of a systematic study of the temperature dependence of the various Mössbauer parameters of synthetic ferri-diopsides, it was observed that for relatively high Fe concentrations in the unfired mixtures of $CaMgSi_2O_6$ (diopside) and α-Fe_2O_3 (hematite), the obtained product after sintering at 1170°C consists of a mixture of ferri-diopside and hematite, the contribution of the latter becoming more and more important as the starting Fe content increases. This limited solubility of α-Fe_2O_3 in $CaMgSi_2O_6$ has been reported before by Huckenholz et al. (1). In analyzing the variable-temperature Mössbauer spectra of these fired diopside/hematite compounds, it was surprisingly established that the hematite phase possesses an unusually high

Morin transition (MT) temperature, and it was therefore decided that the hematite phase must be studied in some detail in the temperature range between 80 and 900 K.

The Morin transition (2) concerns a flip of the spin direction from the [111] axis at low temperatures to the (111) plane at high temperatures and is found to occur at $T_M \approx$ 265 K for pure, single-crystal hematite (3). Below T_M, the magnetic ordering is antiferromagnetic (AF state). Above T_M, the spins are slightly canted with respect to one another. As a result, a small spontaneous magnetic moment perpendicular to [111] is formed and the ordering is called weakly ferromagnetic (WF state). The MT is readily observed by Mössbauer spectroscopy (MS) through the change by a factor of ≈ -2 in the quadrupole shift ε_Q of the Zeeman patterns (4). This change is due to the well-known relation between ε_Q and the angle θ between the direction of the magnetic hyperfine field H_{hf} (which is opposite to the spin direction) and the principal axis of the

---

0022-4596/91 $3.00

electric field gradient (EFG) (5). The latter one coincides with the [111] axis. The MT is further associated with a sudden drop of ≈ 8 kOe in the magnitude of H_{hf} in going from low to high T (4).

The MT is known to shift drastically toward lower T values as a result of lattice defects (e.g., poor crystallinity and small particle dimensions) or most types of ionic substitutions. Simultaneously, the transition is spread out over a more or less broad temperature range ΔT_M in which AF and WF states coexist, and in many cases this coexistence persists down to the lowest temperatures. In contrast, some $4d$ elements (e.g., Rh and Ru) are observed to increase T_M when they substitute for Fe. The same effect seems to occur in the case of Si (6, 7); however, the experimental evidence thereof has hitherto been less convincing. The results of the present study irrefutably show that the MT temperature of the investigated α-Fe$_2$O$_3$ phase exceeds room temperature (RT), and, considering the nature of the sample, a plausible explanation for this finding seems to be the presence of Si in the hematite lattice. However, as will be discussed hereafter, another mechanism can explain the observation as well.

2. Experimental

The sample referred to as FD40 in this work was prepared by heating a mixture of 100 wt% diopside with 40 wt% hematite at 1170°C under atmospheric conditions (8). The resulting product shows a yellow coloration. It was characterized by powder X-ray diffraction (XRD) and scanning electron microscopy (SEM) with energy-dispersive analysis of X-rays (EDAX). [57]Fe Mössbauer spectra at variable temperatures between 80 and 900 K were collected on a time-mode spectrometer with constant acceleration drive and a triangular reference signal. The source matrix was Rh. The absorbers con-

sisted of the powdered sample mixed with very pure carbon or boron nitride and uniformly spread out over the support. Spectra were usually run until an off-resonance count rate of at least 10^6 was reached. The total number of channels was 1024 (unfolded). The velocity scale was calibrated interferrometrically and the velocity increment per channel was approximately 0.045 mm/sec. All isomer shift values quoted hereafter are referenced with respect to metallic iron.

The temperature of the absorber in the range 80–400 K was varied using a commercial cryostat/furnace combination. The indicated temperature was commonly stable to within 0.2 K. Temperatures between 300 and 900 K were obtained in a commercial Mössbauer furnace with similar temperature stability. Temperature scans were done in both ascending and descending sequences. The obtained Mössbauer spectra were analyzed by least-squares fitting of symmetrical, Lorentzian-shaped sextets and doublets to the experimental data. When necessary, additional restrictions were imposed and are mentioned in the next section.

3. Results

The XRD pattern clearly shows the presence of hematite in conjunction with a pyroxene phase and all observed diffraction lines could be ascribed to either of these two compounds. The (104) reflection of the α-Fe$_2$O$_3$ phase, which is well separated from any other XRD line, was found to be slightly broader than that for well-crystallized natural hematite, indicating a mean crystallite diameter of ≈ 500 nm. The corresponding d value of 0.2707 nm is in good agreement with the results for bulk hematites (7).

The SEM images do not allow one to distinguish visually the hematite grains from the diopside ones on the basis of morphological characteristics. The particles have an

ovoid shape with dimensions of the order of 1 μm. The large-area elemental analysis by EDAX is consistent with the known composition of the starting mixture. A large number of grains were scanned individually and at different locations (in the middle and at the edge of the particle) by narrow-beam EDAX with a cross section of $\approx$20 × 20 nm². For some of the spectra, the Fe peak was significantly intensified as compared to the other peaks, indicating that a hematite phase was prominent at the involved location. However, in all these cases the remaining amounts of Mg, Si, and Ca which would explain the respective signals are much too high to be assigned completely to species incorporated into the α-Fe$_2$O$_3$ phase, considering the limited solubility of divalent and tetravalent cations in the hematite lattice. In other words, it was found impossible to isolate in the SEM–EDAX observations the hematite phase from the diopside one and hence to determine its chemical composition.

Mössbauer spectra at some selected temperatures are reproduced in Fig. 1. They consist of a superposition of Zeeman sextets and quadrupole doublets. The latter ones, with total relative area of approximately 50%, arise from ferric and ferrous iron species incorporated in the diopside lattice and are of no importance for the present discussion. The interpretation of these diopside components will be described in detail in a forthcoming paper. In addition to the hematite sextet(s), there is definitely a second magnetic phase present which could be identified from its spectra as magnetite, Fe$_3$O$_4$. Due to its small fraction, it could not be detected in the XRD pattern. Nevertheless, its presence might have important consequences for the magnetization behavior of the sample as reported by Nöller and Knoll (9) since its magnetic moment at RT amounts to 90 emu/g as compared to 0.4 emu/g for α-Fe$_2$O$_3$ (10).

The Mössbauer spectra of pure, single-phase Fe$_3$O$_4$ at temperatures below $T_N \approx$ 870 K consist of two subspectra, arising respectively from iron in tetrahedral (A sites) and octahedral (B sites) coordinations in the spinel lattice. At higher temperatures, the spectrum appears as a broadened singlet, but is actually composed of a singlet from A-site iron and a quadrupole doublet with splitting $\approx$0.15 mm/sec from B-site iron (11).

Because of the small contribution of the magnetite component ($\approx$5% of the total spectral area) and its strong overlap with the more intense hematite and diopside subspectra, it could not be resolved consistently. Therefore, in fitting the spectra the magnetite Mössbauer parameters, except the width Γ, were fixed at their values recently determined by Persoons (11) for a pure Fe$_3$O$_4$ sample at many different temperatures up to 900 K. This procedure might not be entirely correct, but, as seen from the solid lines in Fig. 1, the evaluated line shapes match the experimental ones very closely. Moreover, if the magnetite parameters were forced to have different, but still reasonable, values, the goodness-of-fit of the numerical decomposition did not change markedly and the hyperfine parameters of the other spectral components were not affected significantly. It should be noted that for $T \geq$ 700 K, the magnetite sextets have collapsed into a broad singlet (see Fig. 1e). The shift of T_N to a lower temperature could be due to Ca^{2+} and/or Mg^{2+} substitutions. Both ions are known to substitute to some extent into the magnetite lattice (12, 13) and, since they are both nonmagnetic, they lower the order–disorder transition temperature. Another reasonable explanation is that the magnetite precipitates would have small dimensions so that the large surface area and other defects would lower T_N. The particles could even become superparamagnetic at temperatures below T_N. A combination of several of these features is not unlikely as well.
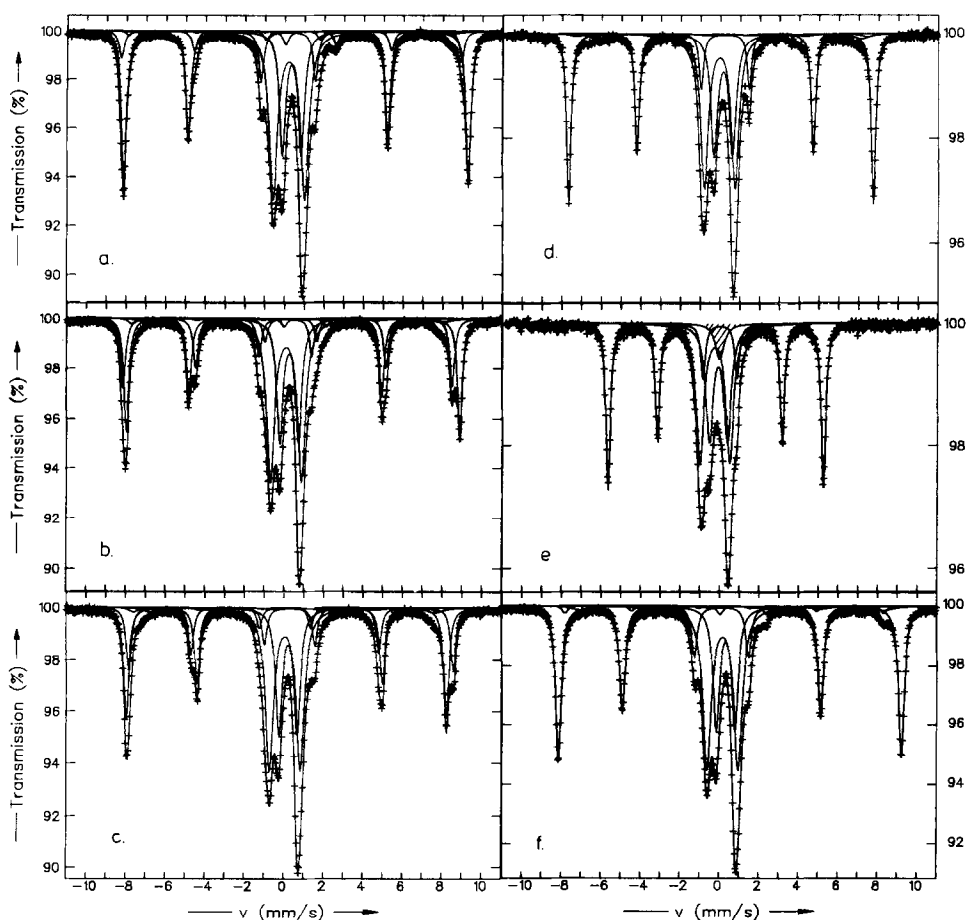
FIG. 1. Mössbauer spectra at some selected temperatures of the sample produced by heating a diopside/ hematite mixture at 1170°C: (a) 80, (b) 300, (c) 380, (d) 480, (e) 800 K. The full lines represent the resolved components (hematite, magnetite, and ferri-diopside) and their sum fitted to the experimental data points. The spectra at 300 and 380 K clearly indicate the coexistence of AF and WF spin states in the hematite phase. The shaded profile in (e) represents the collapsed magnetite component. Spectrum (f) was obtained at 175 K after annealing the sample at 900 K, indicating the absence of a WF component in the hematite contribution.

In a certain temperature interval, the hematite component clearly consists of two subspectra with temperature-dependent relative areas RA. This is clearly illustrated by the 300 and 380 K spectra in Fig. 1 for which the second and the sixth lines are visibly splitted. The two contributions are found to coexist down to 80 K, whereas for $T \geq$ 460 K, only one Fe_2O_3 subspectrum can be resolved. The temperature variations of the evaluated Mössbauer data (relative areas, isomer shifts δ, assumed to be the same for the two components, quadrupole shifts $2\varepsilon_Q$, and hyperfine fields H_{hf}) for the measurements performed at ascending temperatures are summarized in Fig. 2. Their values are
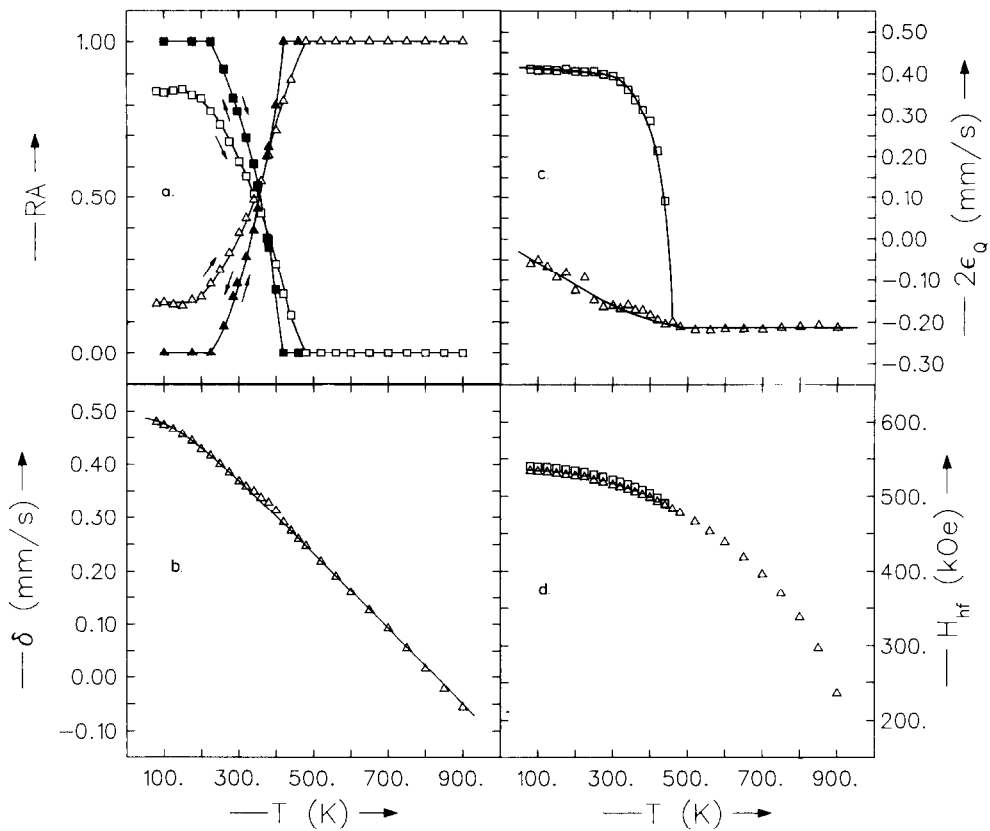
FIG. 2. Temperature variation of the Mössbauer parameters of the hematite phase as measured with ascending temperatures for the as-prepared sample (open symbols); (a) the spectral areas RA relative to total hematite; (b) the isomer shifts δ with calculated dependence shown in full line; (c) the quadrupole shifts $2\varepsilon_Q$; and (d) the magnetic hyperfine fields. Squares refer to AF spin state and triangles to WF spin states. Both states are assumed to have the same δ. Also shown (filled symbols) are the RA values for the descending and a subsequent ascending temperature scan. Full lines in (a) and (c) are meant as a guide for the eye. The dimensions of the symbols do not reflect the errors on the measured quantities.

characteristic for the AF and WF spin states in hematite, and the coexistence of these two states at temperatures below a certain upper limit is believed to be typical for poorly crystalline and/or substituted hematites (14). For the present case, poor crystallinity can be ruled out on the basis of the XRD data. Further, it can be concluded from the rather small line widths (0.30 mm/ sec or less for the outer absorption lines at all temperatures up to 900 K) that the degree

of substitution by Ca^{2+}, Mg^{2+}, or Si^{4+} must be low, say below 5 at.%. Indeed, mentioned cations are all nonmagnetic and hence would cause considerable line broadening when they substitute for Fe.

The MT temperature, $T_{M,a}$ (the subscript a refers to the ascending-temperature sequence), as usual defined as the temperature at which the RA of the AF component is reduced to one-half of its low-temperature saturation value, $RA_{AF}(0)$, is found to be

345 ± 5 K. The width $\Delta T_{M,a}$ of the transition region amounts to $\approx$220 K and is extremely broad compared to previously studied hematites showing similar Mössbauer features (see, e.g., (14) and references therein).

After being heated at 900 K and subsequently cooled down slowly to RT, the sample was again measured at 300 K. The Mössbauer parameters were found to be very close to those obtained from the previous 300 K run, except for RA for which a significant change was observed. In order to study this effect more closely, the sample was brought at 460 K, i.e., above the original MT temperature, and spectra were collected at variable descending temperatures. The results for RA are indicated in Fig. 2a as well. The changes for the other parameters were insignificant and therefore not shown in the drawings. The MT was determined as $T_{M,d} = 354 \pm 5$ K and the width as $\Delta T_{M,d} \approx 160$ K, which is still very broad. As seen from Fig. 2a, no WF spin state is present for $T \leq 260$ K, in contrast to the first series of runs for which RA_{WF} at low temperatures saturated at 16% of the total hematite fraction.

Finally, a third temperature scan was done, this time in the range 100–420 K with ascending temperatures. All Mössbauer parameters, also RA, were found to be exactly in line with the results obtained from the spectra recorded in the descending-temperature scan. From this finding, it can be concluded that the behavior as displayed in Fig. 2a is not due to a hysteresis effect, but rather to structural changes (smaller defect concentration and more homogeneous composition) as a result of the sample having been heated in vacuum at high temperature and subsequently being cooled down gradually in the Mössbauer furnace. One such change is the enrichment of the magnetite phase from $\approx$5% of total iron to $\approx$7.5% at the expense of the hematite fraction. At this point, it should be mentioned that annealing the sample for 16 hr at 1000°C did not result

in any further changes of the Mössbauer parameters at 300 K.

The temperature variation of δ (Fig. 2b) was interpreted following the suggestion of Pound and Rebka (15), writing δ as a sum of the constant intrinsic isomer shift, δ_I, and the second-order Doppler shift which is caused by the nonzero mean square velocity of the Mössbauer nuclei, and hence depends on T. Using the Debije model for the lattice vibrations (5), one obtains a mathematical expression for $\delta(T)$ with two parameters, i.e., δ_I and the characteristic Mössbauer temperature Θ_M. The full-line curve in Fig. 2b is the adjusted variation yielding $\delta_I = 0.609$ mm/sec and $\Theta_M = 450$ K. For the combined second and third scans, $\delta_I = 0.604$ mm/sec and $\Theta_M = 480$ K were found. All experimental δ values were reproduced by the calculations to within 0.005 mm/sec. The values for δ_I are in good agreement with earlier results (0.610 ± 0.005 mm/sec) (7), whereas Θ_M for the as-prepared sample is slightly out of the range 480–520 K, covering most previously determined values for different synthetic and natural hematites. However, it is believed that this deviation bears little, if any, significance.

As explained in an earlier report (14), the variations of the AF and WF quadrupole shifts $2\varepsilon_Q$ with increasing temperature (see Fig. 2c) reflect the gradual changes of the respective spin orientations relative to the trigonal axis. The constant value of 0.42 mm/sec observed for the AF phase below $\approx$250 K implies that at these low temperatures the AF spins remain locked along the [111] axis. In the same temperature range, the WF spins are pulled toward the trigonal axis as T decreases. For the as-prepared sample at 80 K, the angle is $\approx$60° instead of 90° as found for the WF state in single-crystal hematite. Approximately the same canting angle is observed for the WF spins in the annealed sample at the lower temperature limit of their appearance in the spectra, i.e., at $\approx$260 K.
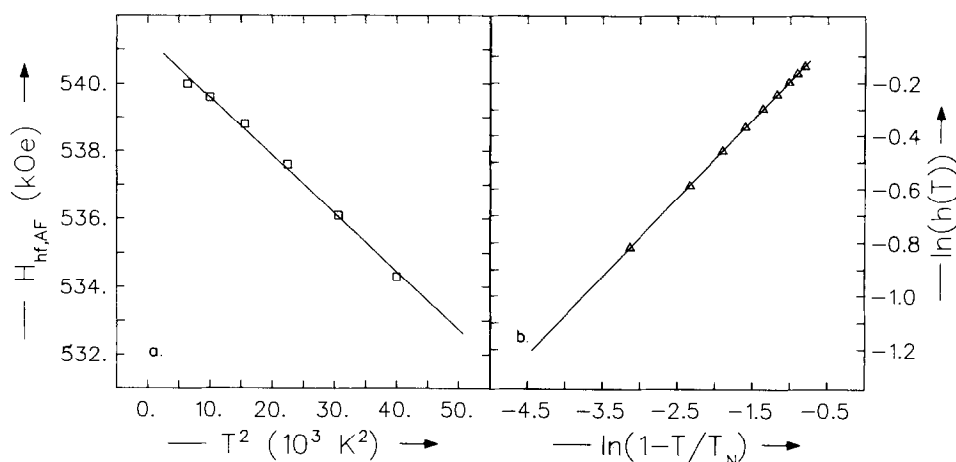
FIG. 3. (a) The low-temperature magnetic hyperfine field of the AF spin state plotted as a function of T^2. The straight line is the adjusted variation based on spin-wave theory. (b) The logarithm of the reduced magnetic hyperfine field $h(T)$ of the high-temperature WF spin state plotted against the logarithm of $(1 - T/T_N)$. The full line is the adjusted linear variation yielding the critical parameters D and β.

The low-temperature variation of the magnetic hyperfine fields can be explained on the basis of the expression for the sublattice magnetization, $m_S(T)$, derived from spin-wave theory by Kubo (*16*) for an ideal two-sublattice antiferromagnet with six nearest-neighbor superexchange paths, each with interaction strength J_e:

$$m_S(T) = 1 - 1.59 \times 10^{-3} (kT/2J_e)^2. \quad (1)$$

Since the reduced hyperfine field, $h(T) = H_{hf}(T)/H_{hf}(0)$, for Fe^{3+} is to a good approximation proportional to $m_S(T)$, H_{hf} should vary linearly with T^2. As shown in Fig. 3a, this was found to be the case for the AF fraction at temperatures below ≈ 260 K (at higher T there is an additional variation due to the gradual rotation of the spins away from the [111] axis), yielding $H_{hf}(0) = 541.0 \pm 0.5$ kOe and $J_e = 35$ K for the as-prepared sample, and $H_{hf}(0) = 544.0 \pm 0.5$ kOe and $J_e = 33$ K for the annealed sample. It is worth mentioning that the presently obtained results for J_e are in reasonable agreement with the value $J_e = 32$ K recently

reported by de Bakker *et al.* (*17*) for an α-Fe_2O_3 sample produced by thermal decomposition of γ-FeOOH at 820 K.

For the high-temperature WF phase, the reduced magnetic hyperfine field was interpreted using the relation

$$h(T) = D(1 - T/T_N)^\beta, \quad (2)$$

which is based on the well-known one-third-power law ($\beta = 0.33$) for the temperature variation of the sublattice magnetization for T approaching T_N. D and β are the so-called critical parameters. According to van der Woude (*4*), for well-crystallized single-phase α-Fe_2O_3, Eq. (2) can be applied throughout the entire temperature interval between T_M and T_N. Assuming the WF saturation field to be 8 kOe less than the AF saturation field (*4, 18*), and adjusting Eq. (2) to the present experimental data in successively broader T intervals, all with upper limit 900 K, an acceptable agreement (i.e., all calculated field values to within 1 kOe equal to the experimental values) was found for $T \geq 520$ K. The results are shown in Fig.

3b in which $\ln(h(T))$ is plotted against $\ln(1 - T/T_N)$. The straight line represents the fit yielding $D = 1.11$, $\beta = 0.30$, and $T_N = 941$ K. The evaluated D and β parameters are in excellent agreement with experimental (4) and theoretical (19, 20) literature data, whereas T_N is somewhat lower as compared to the value measured for pure hematite by MS, i.e., 956 K (4, 21). The smaller T_N would be consistent with the replacement of a minor amount of iron by nonmagnetic ions. From the molecular-field theory of antiferromagnetism (see, e.g., (22)), it is estimated that a substitution of 1.5 at.% is sufficient to explain the observed shift in T_N.

Finally, it should be mentioned that a second sample, with about three times less α-Fe_2O_3 in the unfired mixture, has been measured as well. Like FD40, the sintered material contains a hematite phase; however, its Mössbauer spectrum accounts for only $\approx 10\%$ of the total spectrum and hence its parameters are less accurately determined. Nevertheless, there can be no doubt that for this hematite too the MT takes place at a temperature considerably above that for a pure, single-crystal sample. The larger AF contribution at RT as compared to FD40 (respectively 70 and 60% of total hematite fraction) even suggests that T_M is slightly higher than that of FD40.

4. Discussion

Obviously, the most remarkable and interesting aspect of this study concerns the Morin transition, more precisely the high-temperature T_M at which it occurs, and the extremely broad temperature interval ΔT_M in which it evolves. At present, only two factors are known to exist which cause a shift of the MT to higher T values, i.e., replacement of part of the iron by certain other elements and high pressures.

To the best of the authors' knowledge,

no relevant information with respect to the magnetic properties of Ca^{2+}- or Mg^{2+}-containing α-Fe_2O_3 has ever been reported. However, it is believed that these cations would lower the MT temperature for the following reason. When divalent cations substitute for Fe^{3+}, vacancies or hydroxyl groups have to be introduced in the anionic sublattice in order to maintain charge neutrality. In general, the presence of sufficient amounts of defects or OH^- increases the local lattice spacings (23, 24), i.e., produces a so-called negative pressure, and hence depresses T_M (25). In contrast, when Si^{4+} ions are incorporated into the hematite lattice, then Fe^{2+} ions in the vicinity of these silicons will be formed, and, as discussed in our previous paper on natural hematites, this feature could have a tremendous effect on the MT, of the same order of but opposite to Ti doping, in which case a concentration of 0.3 mole% Ti causes the MT to be depressed to below 12 K (26). To date, however, no quantitative data for well-defined Si-containing α-Fe_2O_3 are available to support the above suggestion.

A second possible explanation for the high T_M is dictated by the fact that no isolated hematite phases could be detected by the narrow-beam EDAX analyses. This could mean that the hematite grains are completely surrounded by the diopside matrix. If this were so, the mismatch between the thermal volume expansion of diopside and hematite (21, 27) could result in a high positive pressure built up on the latter during cooling down of the material. According to the high-pressure Mössbauer work of Bruzzone and Ingalls (28), a pressure of 60 to 70 kbar could explain the measured T_M value. However, for such high pressures a shift in the lattice spacings of $\approx 0.8\%$ as compared to α-Fe_2O_3 at 1 atm would be expected (29), and this was not observed. Therefore, this second interpretation seems to be less likely than that one based on the

incorporation of Si into the hematite lattice. However, further experimental work is needed to rule it out with certainty.

Acknowledgments

References

1. H. G. HUCKENHOLZ, J. F. SCHAIRER, AND H. S. YODER, JR., Mineral. Soc. Am. Spec. Pap. 2, 163 (1969).

2. F. J. MORIN, Phys. Rev. 78, 819 (1950).

3. R. J. FLANDERS AND J. P. REMEIKA, Philos. Mag. 11, 1271 (1965).

4. F. VAN DER WOUDE, Phys. Status Solidi 17, 417 (1966).

5. See, e.g., T. C. GIBB AND N. N. GREENWOOD, "Mössbauer Spectroscopy," 1st ed., Chapman & Hall, London (1971).

6. K. D. JAYASURIYA, A. M. STEWART, AND S. J. CAMPBELL, J. Phys. Chem. Solids 46, 625 (1985).

7. E. DE GRAVE AND R. E. VANDENBERGHE, Phys. Chem. Minerals 17, 344 (1990).

8. R. NÖLLER, PhD thesis, Freien Universität Berlin (1983).

9. R. NÖLLER AND H. KNOLL, Solid State Commun. 47, 237 (1983).

10. M. M. SCHIEBER, in "Selected Topics in Solid State Physics," Vol. VIII, "Experimental Magnetochemistry" (E. P. Wohlfarth, Ed.), p. 158, North-Holland, Amsterdam (1967).

11. R. M. PERSOONS, PhD thesis, University of Gent (1990).

12. J. DE SITTER, A. GOVAERT, E. DE GRAVE, D. CHAMBAERE, AND G. ROBBRECHT, Phys. Status Solidi A 43, 619 (1977).

13. C. DJEGA-MARIADASSOU, T. MERCERON, J. L. DORMANN, M. PORTE, AND P. RENAUDIN, Phys. Status Solidi A 112, 601 (1989).

14. E. DE GRAVE, L. H. BOWEN, R. VOCHTEN, AND R. E. VANDENBERGHE, J. Magn. Magn. Mater. 72, 141 (1988).

15. R. V. POUND AND G. A. REBKA, JR., Phys. Rev. Lett. 4, 274 (1960).

16. R. KUBO, Phys. Rev. 87, 568 (1952).

17. P. M. A. DE BAKKER, E. DE GRAVE, R. E. VANDENBERGHE, L. H. BOWEN, R. J. POLLARD, AND R. M. PERSOONS, Phys. Chem. Minerals, in press.

18. L. TOBBLER, W. KÜNDIG, AND I. SAVIC, Hyperfine Interactions 10, 1017 (1981).

19. E. CALLEN AND H. CALLEN, J. Appl. Phys. 36, 1140 (1965).

20. C. HOHENEMSER, in "Proceedings International Conference on Mössbauer Spectroscopy, Poland–Cracow, 25–30 August 1975" (A. Z. Hrynkiewicz and J. A. Sawicki, Eds.), p. 239, Akademia Gorniczo-Hutnicza, Cracow (1975).

21. C. M. ISERENTANT, G. G. ROBBRECHT, AND R. J. DOCLO, Phys. Lett. 11, 14 (1964).

22. A. H. MORRISH, "The Physical Principles of Magnetism," Wiley, New York (1965).

23. E. WOLSKA AND W. SZAJDA, Solid State Ionics 28–30, 1320 (1988).

24. N. KAWAI, F. ONO, AND K. HIROOKA, J. Appl. Phys. 39, 712 (1968).

25. R. C. NININGER, JR., AND D. SCHROEER, J. Phys. Chem. Solids 39, 137 (1978).

26. N. A. CURRY, G. B. JOHNSTON, P. J. BESSER, AND A. H. MORRISH, Philos. Mag. 12, 221 (1965).

27. M. CAMERON AND J. J. PAPIKE, in "Reviews in Mineralogy," Vol. 7, "Pyroxenes," (C. T. Prewitt, Ed.), Chap. 2, Mineralogical Society of America, Washington DC (1982).

28. C. L. BRUZZONE AND R. INGALLS, Phys. Rev. B 28, 2430 (1983).

29. L. W. FINGER AND R. M. HAZEN, J. Appl. Phys. 51, 5362 (1980).